



Performance Improvement Polyvinylidene Fluoride (PVDF) Mordenite Membranes for Oil-in-Water Emulsion Separation

Brigitta Elga Kusuma Dewi^a, Pranoto Pranoto^a, Ozi Adi Saputra^{b,c}, Edi Pramono^{a*}

^aDepartment of Chemistry, Faculty of Mathematics and Natural Sciences, Sebelas Maret University
Jalan Ir. Sutami 36 A, Kentingan, Surakarta, 57126, Indonesia

^bSustainable Chemical Science and Technology, Taiwan International Graduate Program, Institute of Chemistry, Academia Sinica,
Taipei, 11529, Taiwan

^cDepartment of Chemical Engineering, Collage of Engineering National Taiwan University
Taipei, 10617, Taiwan

*Corresponding author: edi.pramono.uns@staff.uns.ac.id

DOI: 10.20961/alchemy.20.2.82146.226-237

Received 21 December 2023, Revised 27 June 2024, Accepted 28 July 2024, Published 30 September 2024

Keywords:

membrane performance;
mordenite;
oil-in-water emulsion;
PVDF

ABSTRACT. Improving the performance of membranes appropriate for oil-in-water separation is a global challenge. In this study, we prepared a PVDF/Mordenite (PZM) membrane and determined its properties to separate oil-in-water emulsions to address this challenge. The PVDF and PZM membranes were fabricated using the phase inversion technique and applied to separate two types of oil-in-water emulsions 1:99 (wt%), including vegetable oil and used cooking oil emulsion. PVDF polymer with DMAc solvent was added to mordenite with a concentration variation of mordenite. The addition of mordenite did not affect the increase of the β fraction on the hybrid membrane surface but could improve the membrane hydrophilicity. The addition of mordenite in the PVDF membrane has improved the characteristics of the membrane, including water flux, rejection membrane >90%, and FRR up to two times greater than a pristine PVDF membrane. Morphological analysis of the membrane confirmed an asymmetric membrane composed of finger-like and sponge-like. Combining mordenite and PVDF membrane to separate oil-in-water emulsions provides a new approach to oil wastewater treatment.

INTRODUCTION

Waste oil discharged into the environment causes severe environmental pollution to our lives. A huge amount of oil-contaminated water can produce water-in-oil emulsions (W/O) and oil-in-water emulsions (O/W) that can mask oxygen demand (Kuang *et al.*, 2020), and it is crucial to take necessary actions to separate the oil emulsions (Liu *et al.*, 2024). Several conventional separation methods, such as adsorption (Guselnikova *et al.*, 2020), centrifugation, filtration, and flotation, are used to separate oil-in-water emulsions. However, most of them suffer from limitations such as low separation efficiency, expensive, and require a more complicated method (Baig *et al.*, 2022).

Membrane technology was presented as an efficient approach to separate oil-in-water mixtures due to easy processing (Xie *et al.*, 2020) and effective ability to remove oil droplets (Wen *et al.*, 2021). The membranes used to separate oil and water such as polyethersulfone (PES) (Lei and Guo, 2021), polyacrylonitrile (PAN), and polyvinylidene fluoride (PVDF) (He *et al.*, 2021). PVDF has many advantages related to its excellent chemical stability and good ability in engineering processes (Hai *et al.*, 2019). PVDF has been widely used for wastewater treatment (Gao *et al.*, 2021). Superhydrophobic PVDF membranes demonstrate excellent separation of oil-in-water emulsion, but the flux value gradually decreases with increasing cycle time (Ding *et al.*, 2019) and the superhydrophobic nature of PVDF membrane for oil-in-water separation can lead to severe membrane fouling (Tang *et al.*, 2020). Consequently, developing new membrane innovations with a high permeation flux value, high separation efficiency, good antifouling ability, and good mechanical strength are urgently needed for oil-in-water separation applications (Bhalani *et al.*, 2018).

Cite this as: Dewi, B. E. K., Pranoto, P., Saputra, O. A., and Pramono, E., 2024. Performance Improvement Polyvinylidene Fluoride (PVDF) Mordenite Membranes for Oil-in-Water Emulsion Separation. *ALCHEMY Jurnal Penelitian Kimia*, 20(2), 226-237. <https://dx.doi.org/10.20961/alchemy.20.2.82146.226-237>.

Various methods were developed to enhance the hydrophilicity of the PVDF membrane by mixing additives such as inorganic nanoparticles or hydrophilic polymers (Yang *et al.*, 2020). The properties of the composite are enhanced by adding ZnO and Al₂O₃ nanoparticles (Salih and Kadhim, 2023). In recent research, there have been modifications made to PVDF membranes, one of which involves filling the membrane with inorganic materials (Zou *et al.*, 2021) such as TiO₂ and Al₂O₃ (Ni *et al.*, 2021), Silica (Li *et al.*, 2020), and ZrO₂ (Yaacob *et al.*, 2020). Sun *et al.* (2019) succeeded in fabricating a PVDF/SiO₂ composite hollow fiber to improve composite membrane performance. The PVDF/SiO₂ membrane phase inversion method produces a flux value of 3.16 L/m²h/Bar. Yi *et al.* (2011) effectively altered the PVDF membrane using nano-sized TiO₂/Al₂O₃ for oil-in-water emulsion separation. There was also an excellent flux recovery for fouled membranes but decreased permeate flux. In another study, Cui *et al.* (2019) recommended a modification of the PVDF membrane using SiO₂, which displayed great separation efficiency and potential for regeneration to remove oil-in-water emulsion. However, low flux recovery was observed.

Zeolite is a potential material for water purification as well as oil-in-water emulsion separation. PVDF membrane containing zeolite SAPO-34 increased antifouling performance for BSA filtration due to Si and Al content with a hydrophilic skeleton and large pore volume (Vatanpour *et al.*, 2016). Superhydrophobic zeolite membrane via coordination-driven in situ self-assembly was reported by Xie *et al.* (2020a). The results show that it has great separation capacity and is recyclable for controlling oil-in-water emulsions. Meanwhile, research on PVDF/Mordenite membrane application for emulsion separation has not been widely explored. Therefore, in this study, PVDF-mordenite membranes were prepared and analyzed for oil-in-water filtration performance. In this paper, we also analyzed the chemo-physical properties of the membranes, such as their structure and morphology.

RESEARCH METHODS

Materials

Mordenite was obtained from EduLab, and Polyvinylidene Fluoride (PVDF-Solef 1010; Mw 352.000 g/mol) was acquired from Solvay. N-N-dimethylacetamide (DMAc) and polyethylene glycol 400 (PEG400) were purchased from Merck. Commercial vegetable oil (Fortune) and the surfactant Tween-80 were added to prepare the emulsions.

Fabrication of PVDF/ Mordenite Membrane

The dope solution comprises a polymeric material and a solvent. The dope with a total mass of 12 g was prepared by mixing the mordenite, PEG400, and PVDF with DMAc as the solvent and stirred for 24 h at 60 °C. The dope was cast onto a glass plate and soaked in a water-coagulant bath. A solid membrane was obtained, and the membrane was stored in a glycerine solution for further analysis. Table 1 displays the solution composition used to prepare PVDF/Mordenite (PZM), and the PVDF modified with a mordenite was signed as PZM-x.

Table 1. The Dope Composition of PVDF/Mordenite (PZM) Membranes.

Membrane	Composition (wt%)			
	PVDF	Mordenite	PEG400	DMAc
PVDF	18	-	4	78
PZM-0.5%	18	0.5	4	77.5
PZM-1%	18	1	4	77
PZM-2%	18	2	4	76
PZM-3%	18	3	4	75

Making an Oil-in-Water Emulsion

Oil and water were combined in a ratio of 1:99 (wt%) to form an oil-in-water emulsion. The mixture was stabilized with 0.01 mg/mL surfactant Tween 80, and it was sonicated for 30 minutes.

Membrane Characterization

The structure of mordenite material and membrane analysis was performed with an X-ray Diffractometer (XRD-D8 Advance Bruker) at a range of 10° – 90°. Functional groups and polymorph phase identification were analyzed by Attenuated Total Reflectance Fourier Transform Infrared (ATR-FTIR Agilent Cary 600). Morphology and mapping of the element on the membrane were observed with SEM-EDX JEOL Benchtop JCM 700. The

Guerout-Elford-Ferry equation and gravimetric method were used to measure the average pore size and membrane porosity. The membrane sample with a dimension of $2 \times 2 \text{ cm}^2$ was soaked in distilled water for 30 minutes and weighed as the wet weight of the membrane. The membrane was dried in an oven for 24 h at $60 \text{ }^\circ\text{C}$. Membrane's porosity ε was measured by Equation (1) (Almanassra *et al.*, 2023).

$$\varepsilon = \frac{(W_{\text{wet}} - W_{\text{dried}})}{A \times l \times \rho} \quad (1)$$

Where W_{wet} and W_{dried} represent the membrane's wet and dry weights, A is the membrane's dimensional (cm^2), ρ is the water's density (0.998 g/cm^3) at $25 \text{ }^\circ\text{C}$ and l is thickness measured by Mitutoyo dial thickness.

The Equation (2) calculates the average pore size of a membrane (Umam *et al.*, 2023).

$$r = \sqrt{\frac{(2.9 - 1.75\varepsilon) \times 8\eta l_m J_1}{3800 \times \varepsilon \times \Delta P}} \quad (2)$$

Where η is the water viscosity at $25 \text{ }^\circ\text{C}$ ($8.9 \times 10^{-4} \text{ Pa}\cdot\text{s}$), l_m is the wet thickness of the membrane (m), J_1 is the water flux from the membrane ($\text{L/m}^2\text{h}$), ε is the porosity (%), and ΔP is the operating pressure (Pa).

Furthermore, the water and oil contact angles (WCA and OCA) were measured to evaluate the surface properties of the membranes. Water or oil was dripped onto the membrane surface and then recorded using a camera (48 MP magnification $5\times$). The WCA and OCA ($^\circ$) were analyzed using a contact angle plug-in mode in ImageJ software.

Membranes Performance Evaluation

Three significant parameters for filtration membranes in oil emulsion treatment have been identified: pure water flux, membrane rejection, and antifouling (FRR) measurements. The analysis of pure water flux was performed by setting up a membrane with a 5 cm diameter on a Buchner funnel tube. Distilled water was fed into the Buchner funnel, and after 30 minutes of filtration at 0.8 bar of pressure, the flux of pure water was recorded (J_0). Equation (3) was used to determine the water flux (J_1) after the permeate was collected (Xie *et al.*, 2020).

$$J_1 = \frac{v}{A \times t} \quad (3)$$

Where J_1 is water flux ($\text{L/m}^2\text{h}$), v is the permeate volume (L), A is surface area (m^2), and t is time measurement (h).

Using a UV-Vis Spectrophotometer with a wavelength of 229 nm, the concentrations of retentate and permeate were calculated to determine membrane rejection using Equation (4) (Xie *et al.*, 2020).

$$\% R = \left(1 - \frac{C_p}{C_r}\right) \times 100 \quad (4)$$

%R represents the resulting percentage of rejection for oil, permeate concentration is denoted by C_p , and retentate concentration is denoted by C_r .

Flux Recovery Ratio (FRR) was used to assess the membranes' antifouling properties. After the filtration of water and oil emulsion, the membrane was placed on a Büchner funnel, and the feed was filled with distilled water. Equation (5) was used to determine the FRR membrane after the permeate was collected (J_2).

$$\text{FRR} = \frac{J_2}{J_0} \times 100\% \quad (5)$$

RESULTS AND DISCUSSION

Fabrication of PVDF/Mordenite Membrane

PVDF/Mordenite membrane was carried out using the phase inversion method. Membrane characterization using ATR-FTIR is shown in Figure 1. The data result shows that the absorption band at 1070 cm^{-1} is related to the SiO_4 tetrahedron units (Sadrara *et al.*, 2021). The wavelengths 1178 cm^{-1} and 1402 cm^{-1} are related to the vibrations of C-F and C-H stretching (Sun *et al.*, 2019). The characteristic peaks at 840 cm^{-1} were assigned to the β phase (Cui *et al.*, 2015), and characteristic peaks occur at 762 , 795 , and 974 cm^{-1} , indicating the α phase. The addition of mordenite did not affect the polymer phase change. This indicates that mordenite does not appear much on the surface membrane and has a low affinity for water (Bacariza *et al.*, 2018).

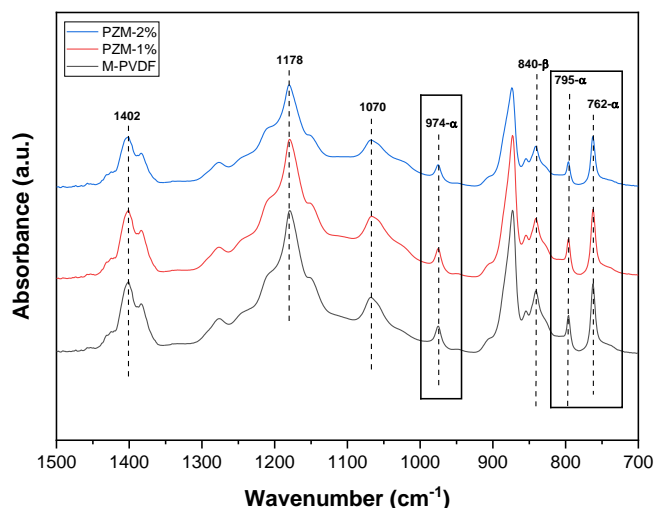


Figure 1. ATR-FTIR spectra Membranes.

The successful composite of mordenite on PVDF membrane was verified using XRD, and the results are displayed in [Figure 2](#). XRD of the PVDF membrane produced a 2θ peak at 18.4° , indicating the α phase. The 2θ peaks with values of 21.43° and 23.50° indicate the β phase of PVDF, which indicates the presence of a polyethylene-like structure. Some typical characteristic peaks in the diffractograms of mordenite and PVDF membranes were confirmed in the diffractograms of PZM-1% and PZM-2% membranes. The diffractogram patterns of PVDF, PZM-1%, and PZM-2% membranes produce 2θ at 18.40° , 21.43° , and 23.50° . The PZM-2% diffractogram shows new peaks 2θ at 13.92° , 22.34° , and 25.70° corresponding to mordenite RRUFF ID No R070524. The diffractogram peak intensity of membrane PZM increases with the addition of mordenite, which indicates that the composite of mordenite on membrane PVDF successfully loaded mordenite into the membrane.

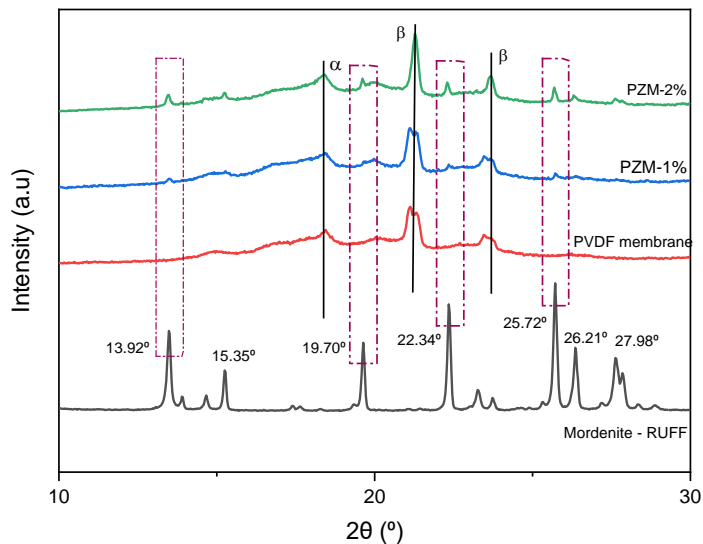


Figure 2. XRD diffractograms of the Mordenite and Membranes.

The Membranes' Hydrophilicity, Porosity, and Average Pore Size

The hydrophilicity of the membranes was evaluated based on the measurement of wettability ([Quinn *et al.*, 2005](#)). The WCA and OCA results are displayed in [Figure 3](#) and [Figure 4](#). The data show that a smaller water contact angle of modified membranes indicates higher membrane surface hydrophilicity. Mordenite has hydrophilic properties and improves water interaction with the membrane surface, which can reduce the WCA ([Petranovskii *et al.*, 2015](#)). Relative hydrophilic properties of pristine PVDF membrane were observed from WCA. It is because PEG contains a dope solution. During phase inversion, PEG attracts PVDF, which is hydrophilic closer to water. As a consequence, the membrane surface becomes more hydrophilic ([Nawi *et al.*, 2020](#)).

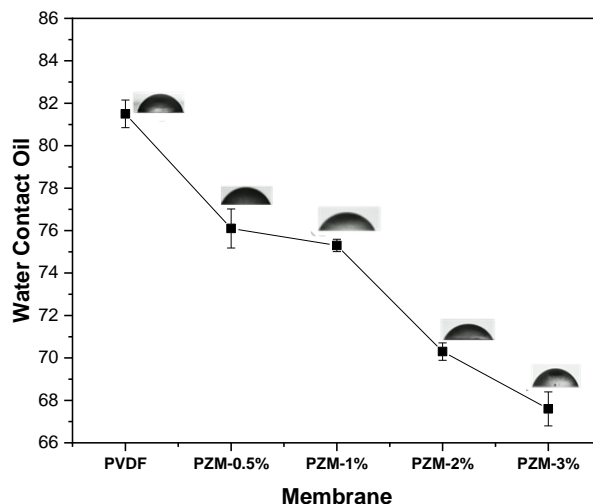


Figure 3. WCA of the Membranes.

The PVDF/Mordenite membranes had a smaller oil contact angle than the pristine membrane, which indicates the addition of mordenite can increase the adhesion force between the emulsion and the surface of the membrane. The increase in adhesion force is due to the impact of the mordenite structure, which has a hydrophilic and hydrophobic backbone (Pal *et al.*, 2022). When the membrane surface was contacted with an oil droplet, introducing mordenite facilitated interaction between membrane and oil producing smaller OCA. The result showed that used cooking oil had a lower Oil Contact Angle (OCA) than vegetable oil.

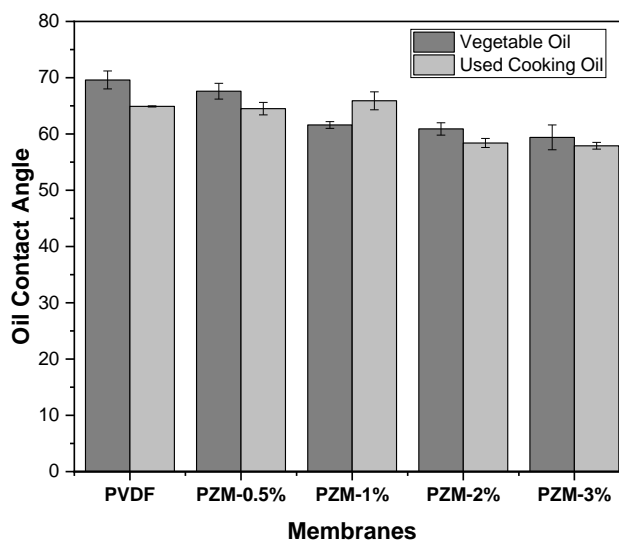


Figure 4. Oil Contact Angle (OCA) Membranes.

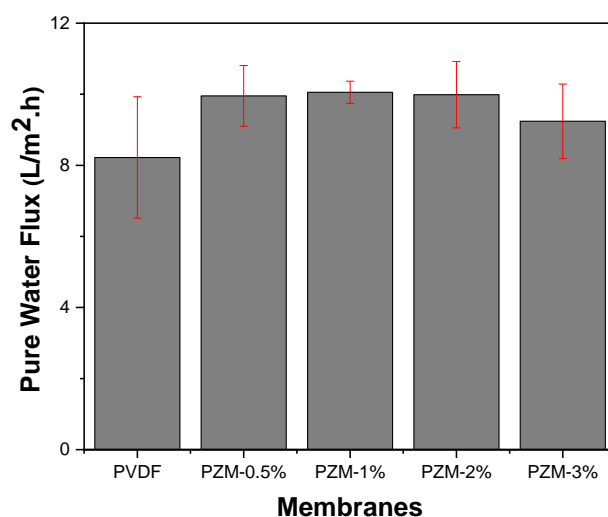
Table 2 presents the membrane's porosity and average pore size. In addition, mordenite enhanced the porosity of the membrane. Instead, the addition of higher filler concentration will result in the creation of additional pores on the membrane's surface so that porosity increases (Méricq *et al.*, 2015). The existence of pores on the membrane's surface is due to the properties of hydrophilic mordenite. The hydrophilic mordenite can produce a repulsion between polymer and filler, therefore causing to increase in porosity. As shown in Table 2, the addition of mordenite affects the decrease in average pore size. However, the average pore size with the mordenite filler remains relatively the same.

Table 2. Membranes's porosity and average pore size.

Membrane	Porosity (%)	Average Pore Size(μm)
PVDF	77.52	0.90
PZM-0.5%	80.92	0.68
PZM-1%	93.52	0.51
PZM-2%	93.54	0.51
PZM-3%	94.66	0.49

Pure Water Flux Analysis

Figure 5 shows the impact of the addition of mordenite concentration on the membrane pure water flux. The pristine PVDF membrane had a smaller water flux than the modified membrane. The smallest pure water flux in the pristine PVDF membrane is 8.22 L/m²h, and the highest value of PZM-1% was 10.06 L/m²h. The addition of mordenite filler can improve water flux. Meanwhile, pure water flux decreased with the addition of 3% mordenite. The factors that affect the increase in pure water flux are porosity and hydrophilicity. The water flux will increase as the hydrophilicity increases because the membrane can interact with water more easily and permeate more quickly (Wang *et al.*, 2021).

**Figure 5.** Pure water flux of the membranes.

Analysis of Membrane Performance Toward Filtration of Oil-In-Water Emulsion

Membrane performance analysis was conducted by filtration of a 100 mg/L oil-in-water emulsion. The mechanism of separating oil-in-water emulsions is by breaking the emulsions. Then, the oil particle is held on the membrane surface so that the membrane surface can miss the water particles. The inclusion of mordenite into the PVDF membrane was able to improve water permeate, as shown in Figure 6. Moreover, by increasing the mordenite content (PZM-0.5% to PZM-2%), the permeate flux of the membrane was significantly increased. The enhancement in permeate flux could be ascribed to the water transport across the membranes. The highest value was achieved by adding 2% mordenite of 8.42 L/m²h.

Furthermore, the water permeate flux in used cooking oil shows the same result as that in vegetable oil. The water permeate flux in used cooking oil increases with the addition of mordenite. The PZM-0.5% membrane shows the lowest permeate flux at 3.36 L/m²h, but the PZM-3% flux increases to 5.03 L/m²h. The water permeate flux in vegetable oil is higher than the water permeate flux in used cooking oil, which may be influenced by the increase in the free fatty acid content in used cooking oil. The high level of free fatty acid indicates that the triglycerides break down into fatty acids, consequently, the oil is increasingly saturated (Huang *et al.*, 2016).

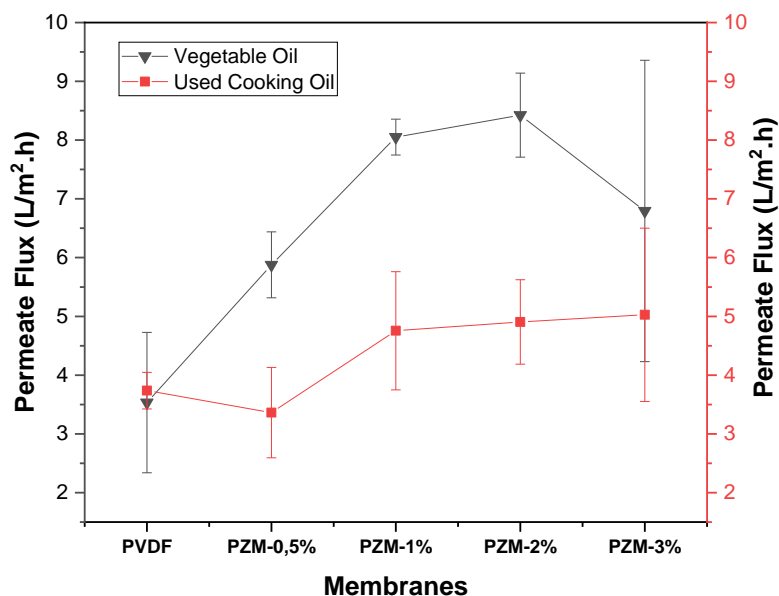


Figure 6. Flux emulsion of the membranes.

The membrane rejection for vegetable oil and used cooking oil emulsion are displayed in Figure 7. The pristine PVDF membrane produces rejection vegetable oil emulsion smaller than the modified PVDF membranes. Among all membranes, the higher rejection rate is approximately 94.28% for PZM-1%, which is two times greater than those pristine PVDF membranes for vegetable oil. The oil rejection percentage of the modified membrane was above 80%, indicating that modification showed good performance for oil removal. The rejection of used cooking oil showed the same result as the rejection of vegetable oil. The rejection value of the pristine PVDF membrane was smaller than that of the modified membranes. The PZM-1% membrane produces the highest rejection of 68.51%.

The result showed a smaller oil rejection of used cooking oil, which corresponds to the permeate flux. In contrast, the low permeate flux water in used cooking oil did not affect the highest rejection percentage. This is because the oil-in-water emulsion for used cooking oil is not emulsified well, so the oil molecules are irregular. Oil emulsions with much smaller droplet sizes can also be filtered by the membrane (Zhang *et al.*, 2021).

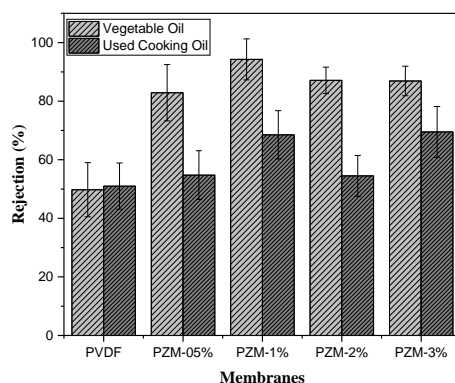


Figure 7. Oil Rejection percentage of the membranes.

To investigate the antifouling performance of membranes was determined by FRR on the rejection of vegetable oil emulsion and used cooking oil. As presented in Figure 8, the pristine PVDF membranes of both emulsions produce lower values than other membranes modified with mordenite, which is less than 60%. Adding mordenite above 1 (wt%) resulted in FRR values of more than 60% for both oil emulsions. The membrane's pore size after filtration could influence the membrane's antifouling properties because the surface of the internal pores could reduce the interaction between oil and the membrane surface. Furthermore, the increased hydrophilicity of the membrane could lessen the attachment of the oil on the membrane surface and, therefore, increase the FRR.

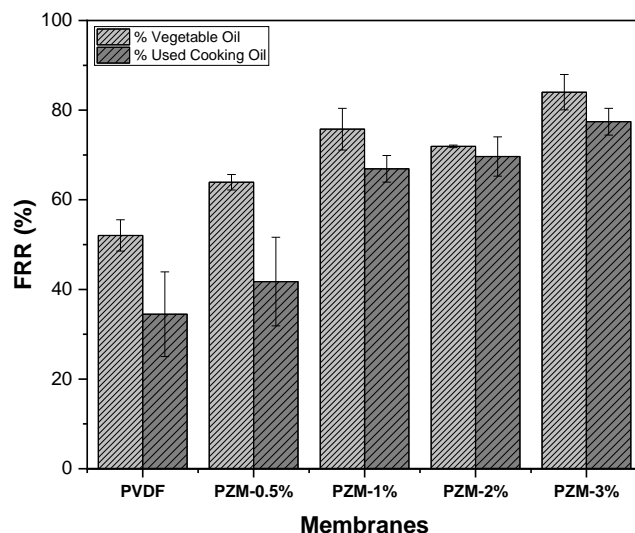


Figure 8. FRR of the membranes.

A comparison of oil rejection and FRR data from prior studies is presented in Table 3. The data indicates that the membrane PVDF/Mordenite is comparable with other research. For instance, PZM has rejected oil-in-water emulsions by 94%, which is higher than PVDF/PDA/PEI, PVDF/HMO, or PVDF/F-VP. The result suggests that the PZM membrane has the potential to be used in the separation of oil-in-water emulsions.

Table 3. Comparative study of rejection and FRR of the PZM with previous studies.

Materials	Method	Rejection (%)	FRR (%)	Reff
PVDF/PDA/PEI	Cross Flow	>85	-	(Xiong <i>et al.</i> , 2020)
PVDF/PDA/MWCNT	Liquid Flow Rate	97.5	90	(Y. Zhang <i>et al.</i> , 2018)
PVDF/HMO	Cross Flow	93	-	(Ismail <i>et al.</i> , 2021)
PVDF/F-VP	Dead-end	>90	93	(Y. Sun <i>et al.</i> , 2019)
PVDF/ZrO ₂ -Multiwalled CNT	Dead-end	95	>80	(X. Yang <i>et al.</i> , 2016)
PVDF/Mordenite (PZM)	Dead-end	94	75.75	This Work

Morphologies of The Membranes

Analysis of membrane morphology is shown in Figure 9. PVDF and PZM-1% membranes were chosen based on membrane performance analysis. Through the phase inversion, the top surface of the pristine PVDF membrane shows a coarser porous structure compared to PZM-1%. The cross-sectional observations are displayed in Figure 9(a) and (b) indicate that the membrane contains finger-like and sponge-like. However, the cross-sectional of PZM-1% had a larger finger-like than the PVDF membrane, which indicates that the PZM-1% membrane performs better than the PVDF membrane. The formation of finger-like pores is due to the addition of PEG and the influence of non-solvent diffusion (Kahrs and Schwellenbach, 2020). The existence of PEG in the composite might accelerate the non-solvent diffusion rate and cause finger-like formation in the membrane structure because it decreases the dope solution's thermodynamic stability (Zhang *et al.*, 2018). As shown in Figure 9, the top surface morphology of the PZM-1% results in a homogeneous distribution of mordenite.

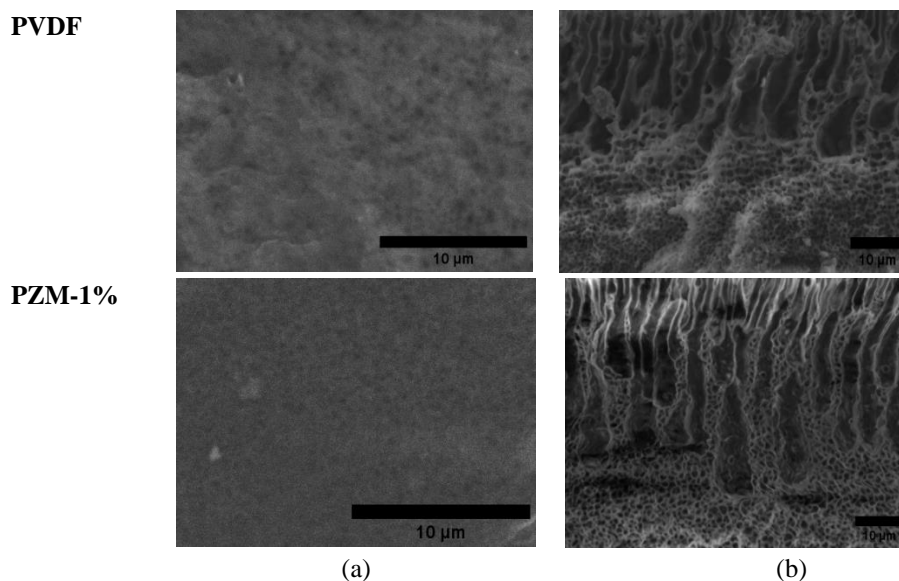


Figure 9. Morphology of (a) Top Surface; (b) Cross Section membrane.

The existence of mordenite in the membrane structure was further confirmed by EDX mapping. **Figure 10(a)** shows the EDX spectra of PVDF membrane representing elements fluorine (F), carbon (C), and oxygen (O). Meanwhile, the presence of mordenite is confirmed in **Figure 10(b)** by the existence of the peak components of Si and Al.

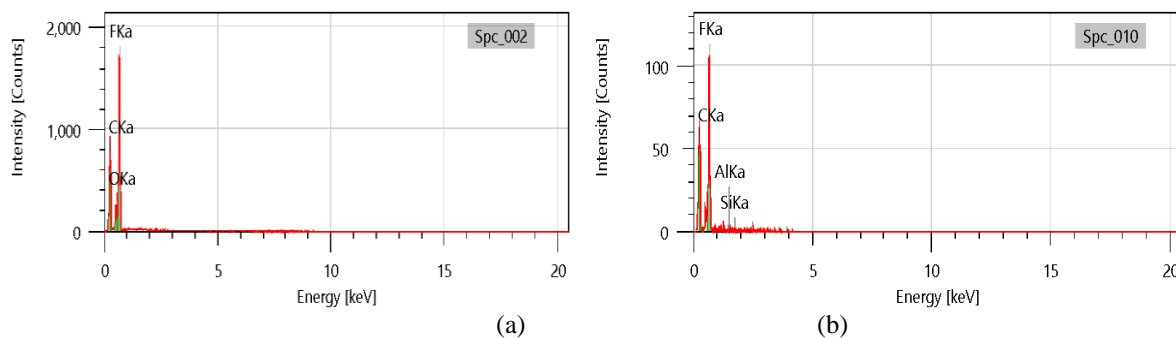


Figure 10. Diffraction EDX (a) PVDF membrane; (b) PZM-1% membrane.

CONCLUSION

Fabrication of PVDF membrane with mordenite was successfully carried out using the phase inversion method. The result of ATR-FTIR indicates α -PVDF and β -PVDF phases, which confirmed for all membranes with a peak at 840 and 763 cm^{-1} . It was strengthened by XRD data indicating α and β phase in $2\theta = 18.4^\circ$ and 21.43° . The addition of mordenite on PVDF membrane decreased WCA and OCA, which indicates a reduction in the hydrophobicity of membranes and increased adhesion force. The result of pure water flux showed that the modification membrane with mordenite increased water permeability to 4.36 $\text{L/m}^2\text{h}$. Due to the molecule size, the permeate water flux in vegetable oil is higher than the permeate water flux in used cooking oil. The rejection of PVDF-modified membrane for vegetable oil emulsion produces a rejection value of more than 80%, while for used cooking oil emulsion, it is more than 54%. FRR analysis showed that compared to other membranes, PZM-3% performed better, increases along with hydrophilicity. Morphological analysis indicated that the pristine membrane produced a smaller finger-like than the PZM-1% membrane. Accordingly, this membrane with mordenite filler showed its potential to be used to filtrate oil-in-water emulsion. This modification of mordenite and PVDF membrane to separate oil-in-water emulsion provides a new approach to wastewater treatment.

CONFLICT OF INTEREST

There is no conflict of interest in this article.

AUTHOR CONTRIBUTION

BEKD: Methodology, Data Analysis and Wrote the Manuscript; PP: Review the Manuscript; EP: Supervised the Experiment and Review the Manuscript.

REFERENCES

- Almanassra, I. W., Jaber, L., Chatla, A., Abushawish, A., Shanableh, A., and Atieh, M. A., 2023. Unveiling the relationship between MOF porosity, particle size, and polyethersulfone membranes properties for efficient decontamination of dye and organic matter. *Chemical Engineering Journal*, 471, 144616. <https://doi.org/10.1016/j.cej.2023.144616>.
- Bacariza, M. C., Graça, I., Lopes, J. M., and Henriques, C., 2018. Enhanced activity of CO₂ hydrogenation to CH₄ over Ni based zeolites through the optimization of the Si/Al ratio. *Microporous and Mesoporous Materials*, 267, 9–19. <https://doi.org/10.1016/j.micromeso.2018.03.010>.
- Baig, U., Gondal, M. A., and Dastageer, M. A., 2022. Journal of Water Process Engineering Oil-water Separation Using Surface Engineered Superhydrophobic and Superoleophilic Membrane for the Production of Clean Water. *Journal of Water Process Engineering*, 45(102473), 1–11. <https://doi.org/10.1016/j.jwpe.2021.102473>.
- Bhalani, D. V., Singh Chandel, A. K., Trivedi, J. S., Roy, S., and Jewrajka, S. K., 2018. High molecular weight poly(vinyl pyrrolidone) induces hierarchical surface morphology in poly(vinylidene fluoride) membrane and facilitates separation of oil-water emulsions. *Journal of Membrane Science*, 566, 415–427. <https://doi.org/10.1016/j.memsci.2018.09.005>.
- Cui, J., Zhou, Z., Xie, A., Meng, M., Cui, Y., Liu, S., Lu, J., Zhou, S., Yan, Y., and Dong, H., 2019. Bio-inspired fabrication of superhydrophilic nanocomposite membrane based on surface modification of SiO₂ anchored by polydopamine towards effective oil-water emulsions separation. *Separation and Purification Technology*, 209, 434–442. <https://doi.org/10.1016/j.seppur.2018.03.054>.
- Cui, Z., Hassankiadeh, N. T., Zhuang, Y., Drioli, E., and Lee, Y. M., 2015. Crystalline polymorphism in poly(vinylidene fluoride) membranes. *Progress in Polymer Science*, 51, 94–126. <https://doi.org/10.1016/j.progpolymsci.2015.07.007>.
- Ding, Y., Wu, J., Wang, J., Lin, H., Wang, J., Liu, G., Pei, X., Liu, F., and Tang, C. Y., 2019. Superhydrophilic and mechanical robust PVDF nanofibrous membrane through facile interfacial Span 80 welding for excellent oil/water separation. *Applied Surface Science*, 485, 179–187. <https://doi.org/10.1016/j.apsusc.2019.04.214>.
- Gao, J., Cai, M., Nie, Z., Zhang, J., and Chen, Y., 2021. Superwetting PVDF membrane prepared by in situ extraction of metal ions for highly efficient oil/water mixture and emulsion separation. *Separation and Purification Technology*, 275, 1–12. <https://doi.org/10.1016/j.seppur.2021.119174>.
- Guselnikova, O., Barras, A., Addad, A., Sviridova, E., Szunerits, S., Postnikov, P., and Boukherroub, R., 2020. Magnetic polyurethane sponge for efficient oil adsorption and separation of oil from oil-in-water emulsions. *Separation and Purification Technology*, 240, 116627. <https://doi.org/10.1016/j.seppur.2020.116627>.
- Hai, A., Durrani, A. A., Selvaraj, M., Banat, F., and Haija, M. A., 2019. Oil-water emulsion separation using intrinsically superoleophilic and superhydrophobic PVDF membrane. *Separation and Purification Technology*, 212, 388–395. <https://doi.org/10.1016/j.seppur.2018.10.001>.
- He, Y., Xu, K., Feng, X., Chen, L., and Jiang, Z., 2021. A nonionic polymer-brush-grafted PVDF membrane to analyse fouling during the filtration of oil/water emulsions. *Journal of Membrane Science*, 637, 119644. <https://doi.org/10.1016/j.memsci.2021.119644>.
- Huang, F., Li, Y., Guo, H., Xu, J., Chen, Z., Zhang, J., and Wang, Y., 2016. Identification of waste cooking oil and vegetable oil via Raman spectroscopy. *Journal of Raman Spectroscopy*, 47(7), 860–864. <https://doi.org/10.1002/jrs.4895>.
- Ismail, N. H., Salleh, W. N. W., Awang, N. A., Ahmad, S. Z. N., Rosman, N., Sazali, N., and Ismail, A. F., 2021. PVDF/HMO ultrafiltration membrane for efficient oil/water separation. *Chemical Engineering Communications*, 208(4), 463–473. <https://doi.org/10.1080/00986445.2019.1650035>.
- Kahrs, C., and Schwellenbach, J., 2020. Membrane formation via non-solvent induced phase separation using sustainable solvents: A comparative study. *Polymer*, 186, 1–20. <https://doi.org/10.1016/j.polymer.2019.122071>.
- Kuang, J., Mi, Y., Zhang, Z., Ye, F., Yuan, H., Liu, W., and Jiang, X., 2020. A hyperbranched Poly (amido amine) demulsifier with trimethyl citrate as initial cores and its demulsification performance at ambient temperature. *Journal of Water Process Engineering*, 38, 101542. <https://doi.org/10.1016/j.jwpe.2020.101542>.
- Lei, J., and Guo, Z., 2021. PES asymmetric membrane for oil-in-water emulsion separation. *Colloids and Surfaces A: Physicochemical and Engineering Aspects*, 626, 127096. <https://doi.org/10.1016/j.colsurfa.2021.127096>.

- Li, K., Wang, K., Zhang, Y., Liu, H., and Wang, J., 2020. A polyvinylidene fluoride (PVDF) – silica aerogel (SiAG) insulating membrane for improvement of thermal efficiency during membrane distillation. *Journal of Membrane Science*, 597, 117632. <https://doi.org/https://doi.org/10.1016/j.memsci.2019.117632>.
- Liu, Y., Bai, T., Zhao, S., Zhang, Z., Feng, M., Zhang, J., Li, D., and Feng, L., 2024. Sugarcane-based superhydrophilic and underwater superoleophobic membrane for efficient oil-in-water emulsions separation. *Journal of Hazardous Materials*, 461, 132551. <https://doi.org/10.1016/j.jhazmat.2023.132551>
- Méricq, J. P., Mendret, J., Brosillon, S., and Faur, C., 2015. High performance PVDF-TiO₂ membranes for water treatment. *Chemical Engineering Science*, 123, 283–291. <https://doi.org/10.1016/j.ces.2014.10.047>.
- Nawi, N. I. M., Chean, H. M., Shamsuddin, N., Bilad, M. R., Narkkun, T., Faungnawakij, K., and Khan, A. L., 2020. Development of hydrophilic PVDF membrane using vapour induced phase separation method for produced water treatment. *Membranes*, 10(6), 1–17. <https://doi.org/10.3390/membranes10060121>.
- Ni, P., Zeng, J., Chen, H., Yang, F., and Yi, X., 2021. Effect of different factors on treatment of oily wastewater by TiO₂/Al₂O₃-PVDF ultrafiltration membrane. *Environmental Technology*, 43(19), 2981–2989. <https://doi.org/10.1080/09593330.2021.1912832>.
- Pal, A., Moldovan, S., Siblani, H. El, Vicente, A., and Valtchev, V., 2022. Defect Sites in Zeolites: Origin and Healing. *Advance Science*, 9(4), 2104414. <https://doi.org/10.1002/adv.202104414>.
- Petranovskii, V., Pestryakov, A., Hernández, M. Á., Rivas, F. C., Claverie, A. L., and Fuentes, S., 2015. Hydrophilicity of Mordenites with Different SiO₂/Al₂O₃ Molar Ratio. *Procedia Chemistry*, 15(646), 72–78. <https://doi.org/10.1016/j.proche.2015.10.011>.
- Quinn, A., Sedev, R., and Ralston, J., 2005. Contact angle saturation in electrowetting. *Journal of Physical Chemistry B*, 109(13), 6268–6275. <https://doi.org/10.1021/jp040478f>.
- Sadrara, M., Khorrami, M. K., Darian, J. T., and Garmarudi, A. B., 2021. Rapid Determination and Classification of Zeolites Based on Si/Al Ratio Using FTIR Spectroscopy and Chemometrics. *Infrared Physics and Technology*, 116, 103797. <https://doi.org/10.1016/j.infrared.2021.103797>.
- Salih, R. M., and Kadhim, H. J., 2023. Nanofiber composite for anti-bacterial application by electrospinning technique. *Kuwait Journal of Science*, 50(3), 262–270. <https://doi.org/10.1016/j.kjs.2023.01.008>.
- Sun, H., Liu, Y., Li, D., Liu, B., and Yao, J., 2019. Hydrophobic SiO₂ nanoparticle-induced polyvinylidene fluoride crystal phase inversion to enhance permeability of thin film composite membrane. *Journal of Applied Polymer Science*, 136(45), 1–12. <https://doi.org/10.1002/app.48204>.
- Sun, Y., Lin, Y., Fang, L., Zhang, L., Cheng, L., Yoshioka, T., and Matsuyama, H., 2019. Facile development of poly(tetrafluoroethylene-*r*-vinylpyrrolidone) modified PVDF membrane with comprehensive antifouling property for highly-efficient challenging oil-in-water emulsions separation. 584, 161–172. <https://doi.org/10.1016/j.memsci.2019.04.071>.
- Tang, F., Wang, D., Zhou, C., Zeng, X., Du, J., Chen, L., Zhou, W., Lu, Z., Tan, L., and Dong, L., 2020. Natural polyphenol chemistry inspired organic-inorganic composite coating decorated PVDF membrane for oil-in-water emulsions separation. *Materials Research Bulletin*, 132, 110995. <https://doi.org/10.1016/j.materresbull.2020.110995>.
- Umam, K., Sagita, F., Pramono, E., Ledyastuti, M., Kadja, G. T. M., and Radiman, C. L., 2023. Polyvinylidene fluoride (PVDF)/surface functionalized-mordenite mixed matrix membrane for congo red dyes removal: Effect of types of organosilane. *JCIS Open*, 11, 100093. <https://doi.org/10.1016/j.jciso.2023.100093>.
- Vatanpour, V., Yekavalangi, M. E., and Safarpour, M., 2016. Preparation and characterization of nanocomposite PVDF ultrafiltration membrane embedded with nanoporous SAPO-34 to improve permeability and antifouling performance. *Separation and Purification Technology*, 163, 300–309. <https://doi.org/10.1016/j.seppur.2016.03.011>.
- Wang, Y., Li, Q., Miao, W., Lu, P., You, C., and Wang, Z., 2021. Hydrophilic PVDF membrane with versatile surface functions fabricated via cellulose molecular coating. *Journal of Membrane Science*, 640, 119817. <https://doi.org/10.1016/j.memsci.2021.119817>.
- Wen, M., Chen, M., Chen, K., Li, P., Lv, C., Zhang, X., Yao, Y., Yang, W., Huang, G., Ren, G., Deng, S., Liu, Y., Zheng, Z., Xu, C., and Luo, D., 2021. Superhydrophobic composite graphene oxide membrane coated with fluorinated silica nanoparticles for hydrogen isotopic water separation in membrane distillation. *Journal of Membrane Science*, 626, 119136. <https://doi.org/https://doi.org/10.1016/j.memsci.2021.119136>.
- Xie, A., Cui, J., Yang, J., Chen, Y., Lang, J., Li, C., Yan, Y., and Dai, J., 2020a. Dual superlyophobic zeolitic imidazolate framework-8 modified membrane for controllable oil/water emulsion separation. *Separation and Purification Technology*, 236, 116273. <https://doi.org/10.1016/j.seppur.2019.116273>.
- Xie, A., Cui, J., Yang, J., Chen, Y., Lang, J., Li, C., Yan, Y., and Dai, J., 2020b. Photo-Fenton self-cleaning

- PVDF/NH₂-MIL-88B(Fe) membranes towards highly-efficient oil/water emulsion separation. *Journal of Membrane Science*, 595, 117499. <https://doi.org/10.1016/j.memsci.2019.117499>.
- Xiong, Z., He, Z., Mahmud, S., Zhou, L., Hu, C., and Zhao, S., 2020. Simple amphoteric charge strategy to reinforce superhydrophilic polyvinylidene fluoride membrane for highly efficient separation of various surfactant-stabilized oil-in-water emulsions. *ACS Applied Materials 7 Interfaces*, 12(41), 47018–47028. <https://doi.org/10.1021/acsami.0c13508>.
- Yaacob, N., Goh, P. S., Ismail, A. F., Aina, N., Nazri, M., Ng, B. C., Nizam, M., Abidin, Z., and Yogarathinam, L. T., 2020. ZrO₂-TiO₂ Incorporated PVDF Dual-Layer Hollow Fiber Membrane for Oily Wastewater Treatment: Effect of Air Gap. *Membranes*, 20(124), 1–17. <https://doi.org/10.3390/membranes10060124>.
- Yang, J., Wang, L., Xie, A., Dai, X., Yan, Y., and Dai, J., 2020. Facile surface coating of metal-tannin complex onto PVDF membrane with underwater Superoleophobicity for oil-water emulsion separation. *Surface and Coatings Technology*, 389, 125630. <https://doi.org/10.1016/j.surfcoat.2020.125630>.
- Yang, X., He, Y., Zeng, G., Zhan, Y., Pan, Y., and Shi, H., 2016. Novel hydrophilic PVDF ultrafiltration membranes based on a ZrO₂-multiwalled carbon nanotube hybrid for oil / water separation. *Journal Material Science*, 51, 8965–8976. <https://doi.org/10.1007/s10853-016-0147-6>.
- Yi, X. S., Yu, S. L., Shi, W. X., Sun, N., Jin, L. M., Wang, S., Zhang, B., Ma, C., and Sun, L. P., 2011. The influence of important factors on ultrafiltration of oil/water emulsion using PVDF membrane modified by nano-sized TiO₂/Al₂O₃. *Desalination*, 281(1), 179–184. <https://doi.org/10.1016/j.desal.2011.07.056>.
- Zhang, R., Sun, Y., Guo, Z., and Liu, W., 2021. Janus Membranes with Asymmetric Wettability Applied in Oil/Water Emulsion Separations. *Advance Sustainable Systems*, 5(5), 1–19. <https://doi.org/10.1002/adsu.202000253>.
- Zhang, Y., Tong, X., Zhang, B., Zhang, C., Zhang, H., and Chen, Y., 2018. Enhanced permeation and antifouling performance of polyvinyl chloride (PVC) blend Pluronic F127 ultrafiltration membrane by using salt coagulation bath (SCB). *Journal of Membrane Science*, 548, 32–41. <https://doi.org/10.1016/j.memsci.2017.11.003>.
- Zou, D., Jeon, S. M., Kim, H. W., Bae, J. Y., and Lee, Y. M., 2021. In-situ grown inorganic layer coated PVDF/PSF composite hollow fiber membranes with enhanced separation performance. *Journal of Membrane Science*, 637, 119632. <https://doi.org/10.1016/j.memsci.2021.119632>.